Received: 22 April 2019 | Revised: 30 June 2019 | Accepted: 1 July 2019

DOI: 10.1002/eng2.12027

RESEARCH ARTICLE

WILEY

A 1D mean line model for centrifugal compressors with variable inlet guide vanes

Brett Dewar[1] | **Mike Creamer**[2] | **Mariana Dotcheva**[1] | **Jovana Radulovic**[1] | **James M. Buick**[1]

[1]School of Engineering, University of Portsmouth Anglesea Building, Portsmouth, UK

[2]Business Edge, Waterlooville, UK

Correspondence
Brett Dewar, School of Engineering, University of Portsmouth Anglesea Building, Portsmouth PO1 3DJ, UK.
Email: brettdewar1@gmail.com

Funding information
Innovate UK, Grant/Award Number: KTP009973

This paper considers a 1D in-line analytical model for centrifugal compressors with variable inlet guide vanes. A theoretical 1D model is developed to predict the effect of varying the inlet guide vane angle at different rotational speeds. An iterative algorithm is presented, which provides a fast and efficient method for evaluating the performance of the compressor under different operating conditions. The results from the analytical 1D model are presented and compared to full 3D CFD (computational fluid dynamics) simulations. The simulations validate the assumptions used in the 1D model and show good agreement between the two approaches over a range of vane angles. Qualitatively, both demonstrate the same trends as the vane angle and rotational velocities are varied. Quantitatively, the pressure ratio was found to agree within 8% and the temperature gain to within 15%. The 1D model was then modified to introduce a 5% loss in the diffuser and this was found to improve the 1D model predictions, with the pressure within 2% of the CFD value.

KEYWORDS

compressor, fluid mechanics, numerical methods, turbomachinery

1 | INTRODUCTION

Centrifugal compressors and pumps are widely used in a range of industrial applications such as refrigeration and air conditioning, turbo-machinery, power generation, and turbochargers. While a compressor can be designed with a particular operating condition in mind, it is often necessary to run the compressor over a wide flow range. Thus, off-design performance and efficiency are often an important consideration. The mass flow rate, and consequently the pressure change across the compressor, can be controlled by adjusting the rotational velocity of the impellers; however, this may not be efficient, particularly if frequent adjustments are required. An alternative approach is the application of Inlet Guide Vanes (IGVs). A positive vane angle produces preswirl in the direction of impeller rotation and, thus, reduces compressor work at a given revolutions-per-minute (RPM).[1]

NOMENCLATURE: α, Absolute flow angle in diffuser; β, Blade angle; γ, Heat capacity ratio; ε, Relative total pressure loss in the diffuser; φ, IGV angle; ρ, Density; Ω, Rotational speed; a, Speed of sound; h, Enthalpy; i, Index for stage through compressor; k, Rotation index; $\dot{m}$, Mass flow rate; p, Static pressure; p_t, Total pressure; r_a, IGV nacelle radius; r_b, IGV radius; r_{diff}, Diffuser radius; r_h, Hub radius; r_{imp}, Impeller radius; r_m, Mean radius at stage; r_s, Shroud radius; s, Entropy; A, Cross-sectional area; C, Absolute velocity; C_U,Component of C in direction of U; M, Mach number; T, Static temperature; U, Tangential velocity; V_m, Meridional velocity; W, Relative velocity; W_U, Component of W in direction of U.

Unlike circumferential pumps, where the applications of IGVs has been limited due to the potential deterioration of the cavitation performance,[2,3] IGVs have been widely introduced to centrifugal compressor inlets[4,5] as a means of varying mass flow rate and pressure-ratio while maintaining a constant rotational speed, and of introducing preswirl into the flow prior to the flow entering the compressor. Early experimental and computational fluid dynamics (CFD) studies[4,6] showed that introducing preswirl increases the efficiency at lower mass flow rates and improves the surge limit. More recent studies have applied CFD simulations to investigate features such as performance,[7,8] unsteady interactions between the IGVs and the impellers,[9,10] pressure fluctuations at large IGV angles,[11] and the effect of IGV geometry.[1,12] A review of preswirl in from IGVs can be found in the work of Liu et al.[13]

Both experimental[14-16] and numerical[3,9,17-22] approaches have been used to study compressor flow, with and without IGVs. Both can give valuable insight; however, both have their limitations. Experimental studies require extensive measurement rigs, often with sophisticated and expensive measuring apparatus, and testing a range of designs can require multiple test-components to be constructed. The flexibility of CFD, where designs can be changed at the click of a mouse, is often considered to overcome some of the issues associated with experimental studies; however, the complexity of CFD models requires long simulation times, due to the high-speed compressible nature of flow through a rotating compressor. Increases in computational power are often applied to improve the resolution and accuracy of a CFD simulation, rather than bringing down the simulation time, which is often measured in days. Thus, there is a need for a simplified tool, which can be applied to give an understanding of the operation of a compressor in different operating conditions, which takes into account the effects of IGV. This is realized on the 1D model presented here.

In this paper, we consider a 1D mean line analytic code, which provides a simple and fast method to predict performance basics. In Section 2, the underlying theory and the numerical algorithm are described. Results for the model are considered in Section 3, where the model is compared to a 3D CFD simulation in Ansys CFX, to evaluate the model assumptions and the overall model performance. The results are discussed in Section 4 and the conclusions are presented in Section 5. The operating conditions chosen for analysis are at, or close to, design operating conditions to minimize the possible effects of choke and surge.

2 | NUMERICAL MODEL

The geometry of the compressor is set out below in Figure 1 as well as the four stations where the fluid properties will be considered. Before describing the details of the numerical model in Section 2.2, it is beneficial to consider the thermodynamics and flow properties at the four stations.

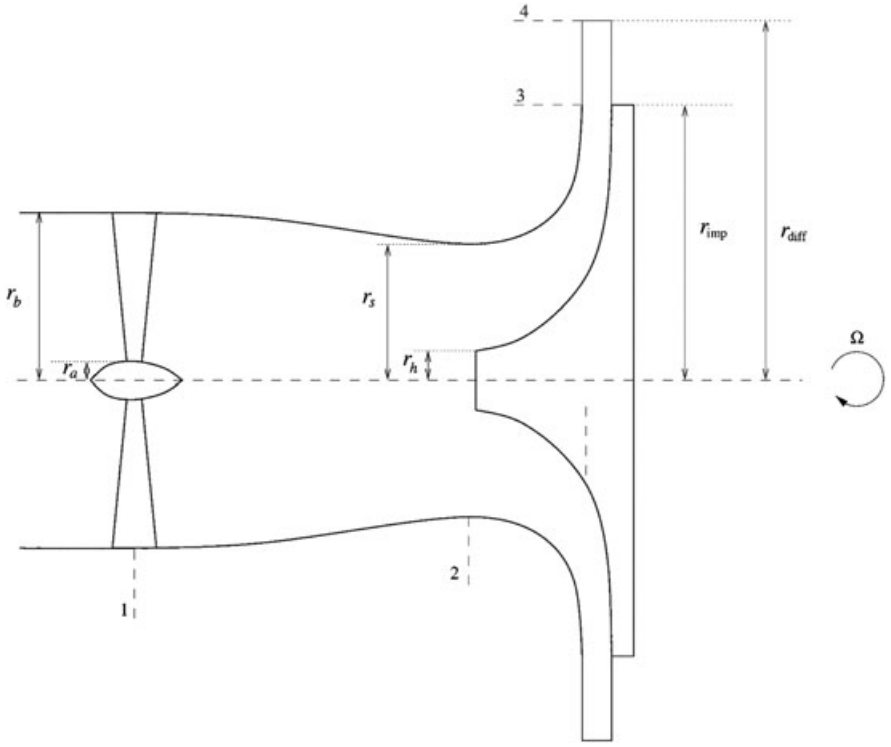

FIGURE 1 Compressor geometry and the 4 stages considered in the 1D model

2.1 | Thermodynamic and flow properties

Consider first the case where the angle of the vane, φ, is zero and so no swirl is imposed on the flow and the initial velocity is in the axial direction. Stage 1 is at the inlet vanes where the initial pressure and temperature are p_1 and T_1, respectively. From tabulated thermodynamic properties of the fluid in the compressor, the enthalpy h_1 and the entropy s_1 can be found, the density is given by the equation of state $\rho_1 = p_1/RT_1$. The mass flow rate, for a rotational angular velocity of the compressor Ω, is given by

$$\dot{m}_1 = \dot{m}_{01}\left(\frac{\Omega_1}{\Omega_0}\right)^k, \tag{1}$$

where $\dot{m}_{01}$ is the known mass flow rate for a rotational speed of Ω_0 and k is the index.

At stage 2, neglecting any losses, we have $p_2 = p_1$, $T_2 = T_1$, $s_2 = s_1$, $h_2 = h_1$, $\dot{m}_2 = \dot{m}_1$, and $\rho_2 = \rho_1$. The magnitude of the absolute velocity is determined from the mass flow rate as

$$C_2 = \frac{\dot{m}_2}{\rho A_2}, \tag{2}$$

and the magnitude of the tangential velocity is

$$U_2 = \Omega r_{m2}, \tag{3}$$

where r_{m2} is the mean radius at stage 2.

Given that these two velocities are perpendicular, the magnitude of the velocity, relative to the rotating impeller, $W2$, is given by

$$W_2 = \sqrt{U_2^2 + C_2^2}. \tag{4}$$

If p_3 is the static pressure at stage 3 and we assume an isentropic process ($s_3 = s_2$), then the density ρ_3, enthalpy h_3, temperature T_3, and heat capacity ratio γ_3 can be determined from tabulated values The tangential velocity of the blades is

$$U_3 = \Omega r_{\text{imp}}, \tag{5}$$

and the relative velocity, W_3, can be found from

$$h_3 - h_2 = \frac{1}{2}\left(U_3^2 - U_2^2\right) + \frac{1}{2}\left(W_2^2 - W_3^2\right). \tag{6}$$

From Figure 2, the meridional velocity V_{m3} is given by

$$V_{m3} = W_3 \sin\beta, \tag{7}$$

where β is the angle of the blade.

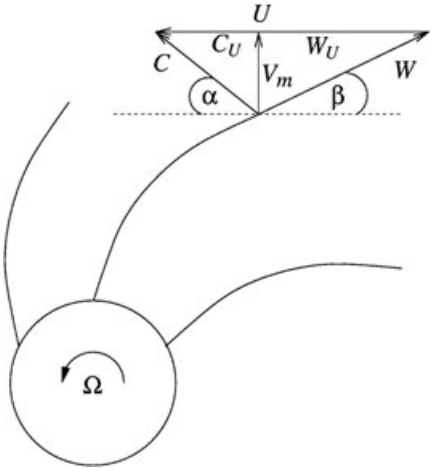

FIGURE 2 Details of the velocities at the tip of the impeller

The mass flow rate at stage 3 is thus

$$\dot{m}_3 = A_3 \rho_3 V_{m3}, \tag{8}$$

with continuity requiring $\dot{m}_3 = \dot{m}_1$.

Moreover, from Figure 2, we note that the tangential velocity U can be expressed as

$$U = C_U + W_U, \tag{9}$$

where C_U and W_U are respectively the absolute values of the absolute velocity and the relative velocity projected onto the tangential velocity, that is,

$$C_U = C\cos\alpha, W_U = W\cos\beta. \tag{10}$$

Thus, from Figure 2, we see that

$$\alpha = \tan^{-1}\left(\frac{V_m}{C_U}\right) = \tan^{-1}\left(\frac{V_m}{U - W_U}\right), \tag{11}$$

and

$$C = \frac{V_m}{\sin\alpha}. \tag{12}$$

Applying this at station 3 gives an expression for C_3. The Mach number at stage 3 is given by

$$M_i = \frac{C_i}{a_i}, \tag{13}$$

where

$$a_i = \sqrt{\gamma_i T_i R}, \tag{14}$$

with $i = 3$. The total pressure at stage 3 is

$$p_{ti} = p_i\left(1 + \frac{\gamma_i - 1}{2}M_i^2\right)^{\frac{\gamma_i}{\gamma_i - 1}}, \tag{15}$$

again with $i = 3$.

Moving to stage 4 at the diffuser outlet. If the static pressure here is p_4, then, again, assuming an isentropic process with $s_4 = s_1$, ρ_4, γ_4, and T_4 can be found, whereas continuity gives $\dot{m}_4 = \dot{m}_3$ and we can assume that $\alpha_4 = \alpha_3$. Here,

$$V_{m4} = \frac{\dot{m}_4}{A_4\rho_4}, \tag{16}$$

and the absolute velocity is

$$C_4 = \frac{V_{m4}}{\sin\alpha_4}. \tag{17}$$

The total pressure at stage 4 is given through Equations (13)-(15) with $i = 4$.

Now, turning our attention to the case $\varphi > 0$. For small angles, we can assume that the flow does not stall and the flow follows the blades such that swirl is introduced with a tangential component to the absolute velocity

$$C_{U1}(\varphi) = V_1 \sin\varphi. \tag{18}$$

Then, at stage 2, applying a free vortex model, we get

$$C_{U2}(\varphi) = \frac{r_1}{r_2}C_{U1}(\varphi). \tag{19}$$

Assuming that p_3 is independent of φ N[23] and that the swirl is carried through the impellers, then the tangential velocity vector, U, in Figure 2 must be offset by an amount $C_{U2}(\varphi)$ in the direction of blade tip motion, whereas β, which is the impeller blade angle, must remain fixed. This is shown in Figure 3, where the φ-dependent variables are shown as solid lines and the φ-independent velocities from Figure 2 are shown as dotted arrows. Note that the magnitude of $C_{U2}(\varphi)$ is exaggerated in Figure 3 later to aid visualization.

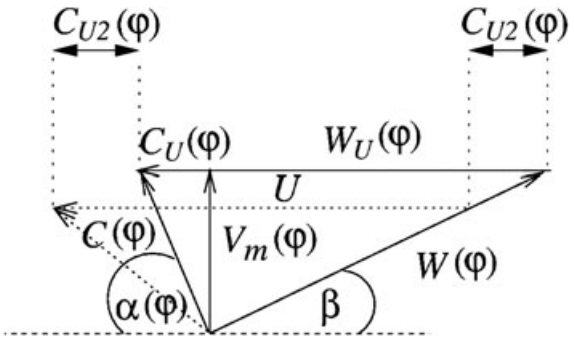

FIGURE 3 Impeller velocities for a vane angle φ

From Figure 3, we see that

$$W_{U3}(\varphi) = W_{U3}(0) - C_{U2}(\varphi), \tag{20}$$

where W_{U3} is now a function of φ and $W_{U3}(0)$ is the value calculated using Equation (10) when $\varphi = 0$. Similarly,

$$C_{U3}(\varphi) = C_{U3}(0) + C_{U2}(\varphi) \tag{21}$$

and

$$V_{m3}(\varphi) = W_{U3}(\varphi)\tan\beta. \tag{22}$$

From these values of $C_3(\varphi)$ and $\alpha(\varphi)$, we can find

$$C_3(\varphi) = \sqrt{V_{m3}^2(\varphi) + C_{U3}^2(\varphi)}, \tag{23}$$

where

$$\alpha(\varphi) = \tan^{-1}\left(\frac{V_{m3}(\varphi)}{V_{U3}(\varphi)}\right). \tag{24}$$

Now, the φ-dependent total pressure $p_{t3}(\varphi)$ can be found from Equations (13)-(15) for $i = 3$ using the appropriate φ-dependent variables.

For the $\varphi > 0$ case, the properties at the end of the diffuser, stage 4, satisfy the same equations as the $\varphi = 0$ case but using the φ-dependent terms $V_{3m}(\varphi)$, $C_3(\varphi)$, and $\alpha_3(\varphi)$.

2.2 | Numerical model

The description of the flow given in Section 2.1 requires the static pressures p_3 and p_4 to be known; however, these values are unknown and must be determined. In both cases, this is performed using an iterative method to determine p_3 such that $\dot{m}_3 = \dot{m}_2$ and p_4 such that the total pressure is either conserved, or reduced due to losses in the diffuser. The numerical model was implemented in MATLAB and is outlined in the flow diagrams in Figure 4.

It predicts the output variables (pressures and velocities) at the outlet from the diffuser, stage 4, (as well as at the internal stages) for a range of rotational speeds fringing from $\Omega_{\min}$ to $\Omega_{\max}$ for a range of vane angles from 0 to $\varphi_{\max}$. The input values are the geometrical variables shown in Figure 1, the initial pressure, p_1, and the thermodynamic properties of the working fluid. A further input is the mass flow rate at a fixed rotational speed Ω_0, for use in Equation (1), where a value of $k = 0.7$ was found to be appropriate.

In the flow chart, an initial guess at p_3 is taken to be p_2 and the mass flow rate $\dot{m}_3$ is calculated. The guess value for p_3 is then incremented in steps of Δp_3 until the correct value of $\dot{m}_3$ (equal to $\dot{m}_1$) is achieved. At each pressure increment, the thermodynamic properties are determined from *REFPROF* software.[24] Good resolution was achieved by setting $\Delta p_3 = p_1/500$; however, in practice, this leads to slow convergence. This was overcome by using an initial guess of

$$p_1\left(\frac{\Omega}{\Omega_{\min}}\right)^k, \tag{25}$$

and allowing larger increments based on the difference between $\dot{m}_1$ and guess-based $\dot{m}_3$. The details of this procedure will depend on the specific details of the compressor being modeled and so are not included here.

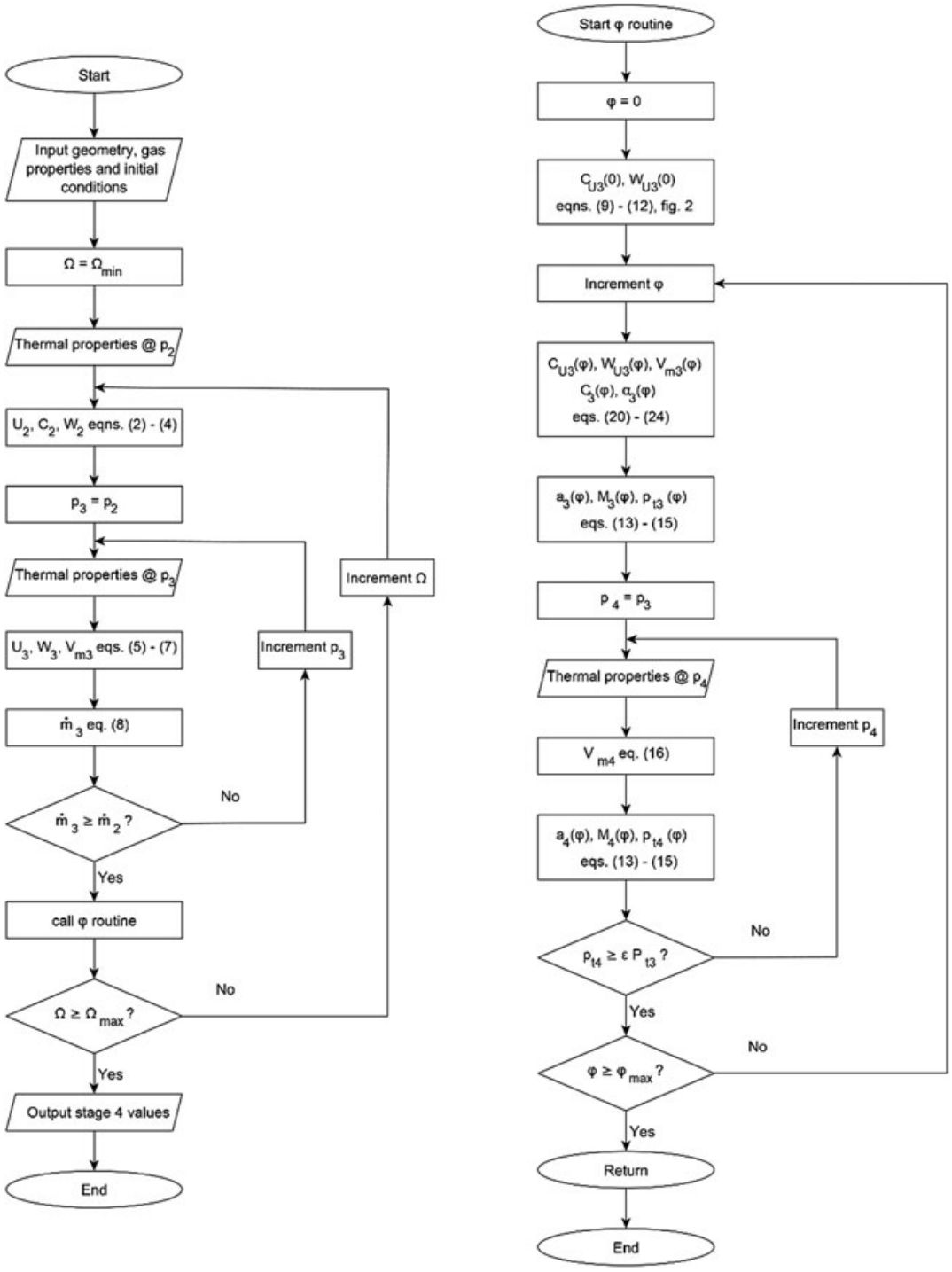

FIGURE 4 Flow chart for the analytical model

A similar iterative approach was adopted to find p_4, where an initial guess was taken to be p_3 and the incremental step, Δp_4, was taken to be $p_3/1000$. The final value of p_4 was obtained when the total pressure at the diffuser outlet, p_{t4} is equal to $\varepsilon p_{t3,}$ where ε represents the diffuser losses. The iteration was performed over the range of φ and Ω values.

3 | RESULTS

To validate the use of the model described above, CFD simulations were performed for comparison. A brief summary of the CFD model approach is included here, full details of the numerical approach, including model validation, are given in

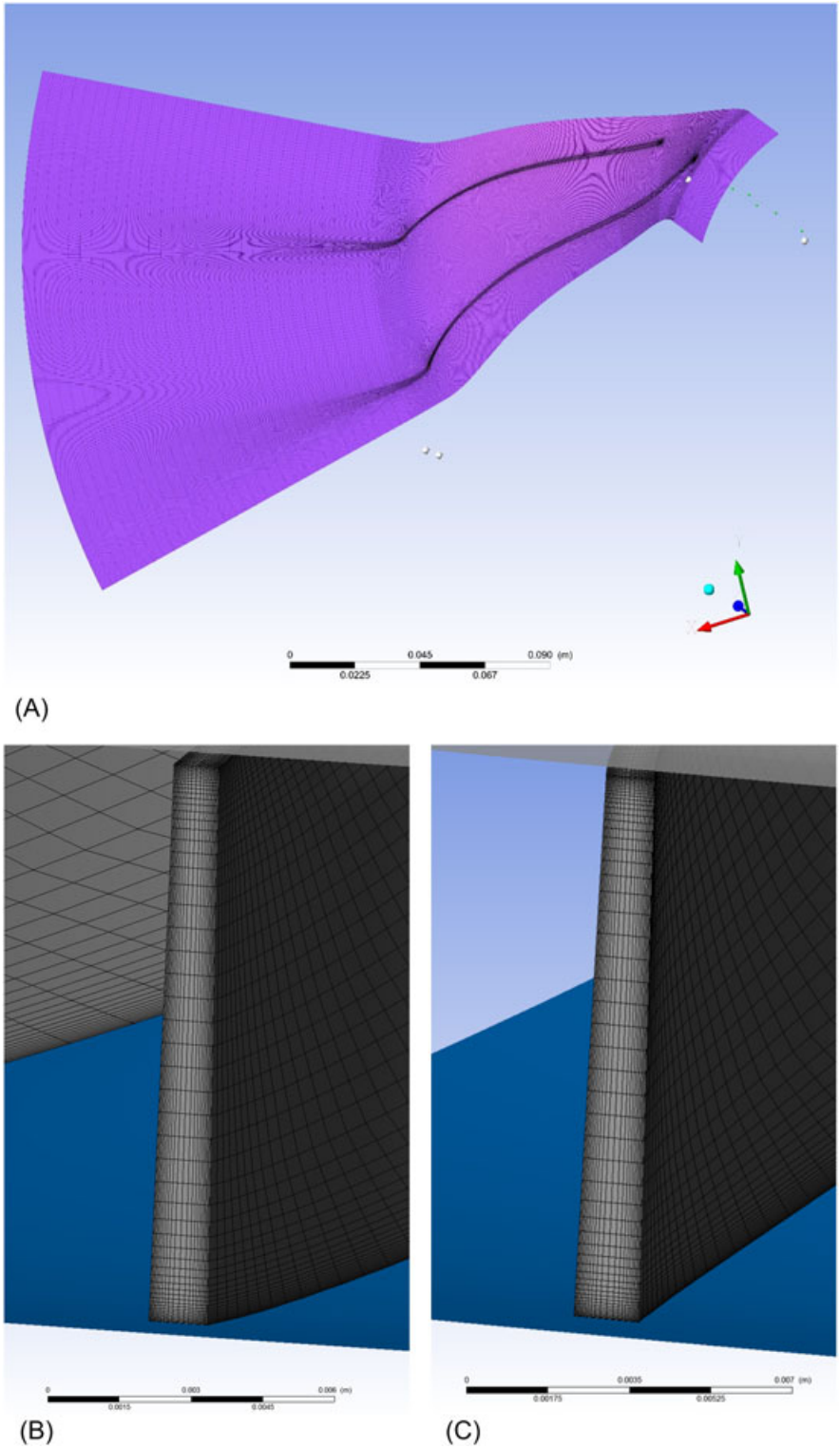

FIGURE 5 Computational fluid dynamics mesh. A, Full mesh; B, Main blade trailing edge; C, Splitter blade trailing edge

the work of Dewar et al.[25] Simulations were performed using the commercial software package ANSYS CFX, version 17.1, for an impeller with 7 full and splitter blades with a k-ω SST turbulence model. The computational domain was partitioned into a stationary inlet, a rotating impeller, and a stationary vaneless diffuser, with frozen rotor interfaces applied between the domains. To save computational resources, an impeller volume consisting of one full blade and one splitter blade was simulated, along with the corresponding volumes in the inlet and diffuser, and periodic boundary conditions were applied in the middle of the blade passages. The simulation mesh was made up of approximately 30 million elements, and the mesh is shown in Figure 5.

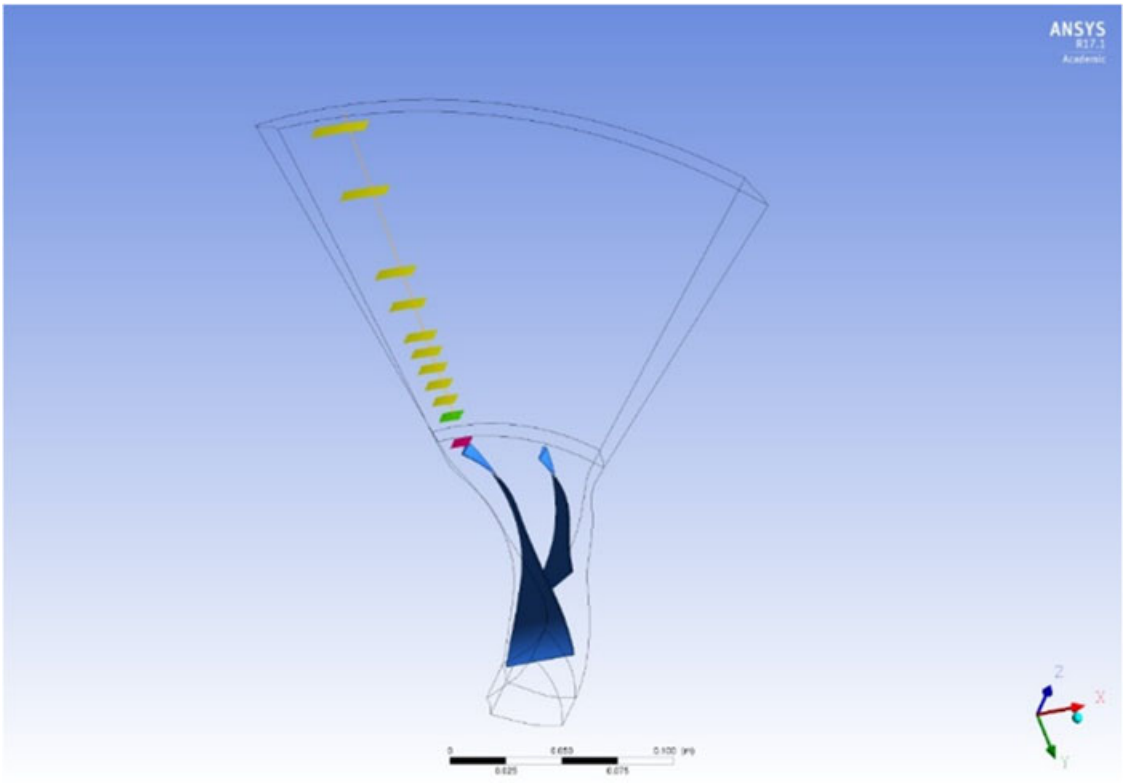

FIGURE 6 The planes used to find α in the diffuser

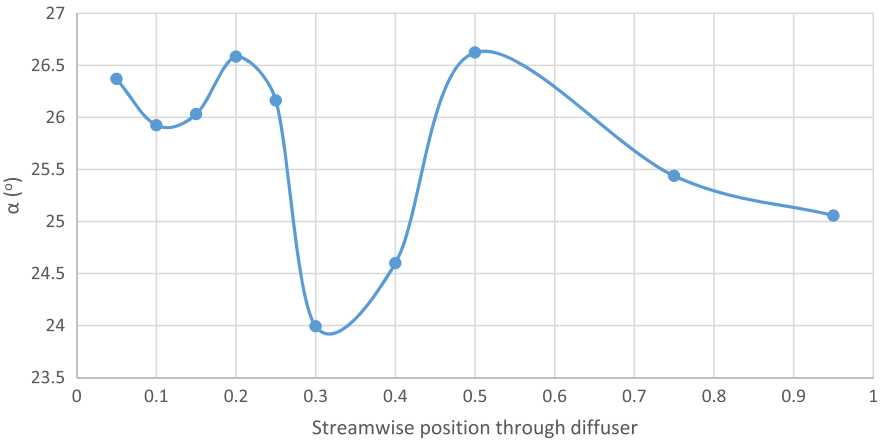

FIGURE 7 Variation in the angle α through the diffuser region

An initial pressure of 259 kPa and initial temperature of 283 K were applied at the inlet. Simulations were run at the design speed of 12 000 RPM as well as at 13 000 and 14 000 RPM at a design speed mass flow rate of $\dot{m}_1 = 2.3$ kg/s.

The CFD simulations were performed on the Sciama High Performance Compute (HPC) cluster at the University of Portsmouth, where a typical run-time was 2 to 3 hours when running on 256 nodes. In contrast, the 1D model ran in under a minute on a standard laptop.

Before comparing the 1D analytical model to the 3D CFD simulation, it is interesting to investigate the main assumption used in the analytical model that the angle α is assumed to be constant through the diffuser with $\alpha_4 = \alpha_3$. To investigate this, the angle was found on a series of planes through the diffuser, as shown in Figure 6.

The values of α on each of the surfaces is shown in Figure 7, which shows the angle remaining approximately constant between 24° and 26.5°. This validates the assumption in the model and also compares well with the value from the analytical model, which was 24.1°.

A comparison of the CFX and analytical results are shown in Figures 8 and 9 for the case $\varepsilon = 1$.

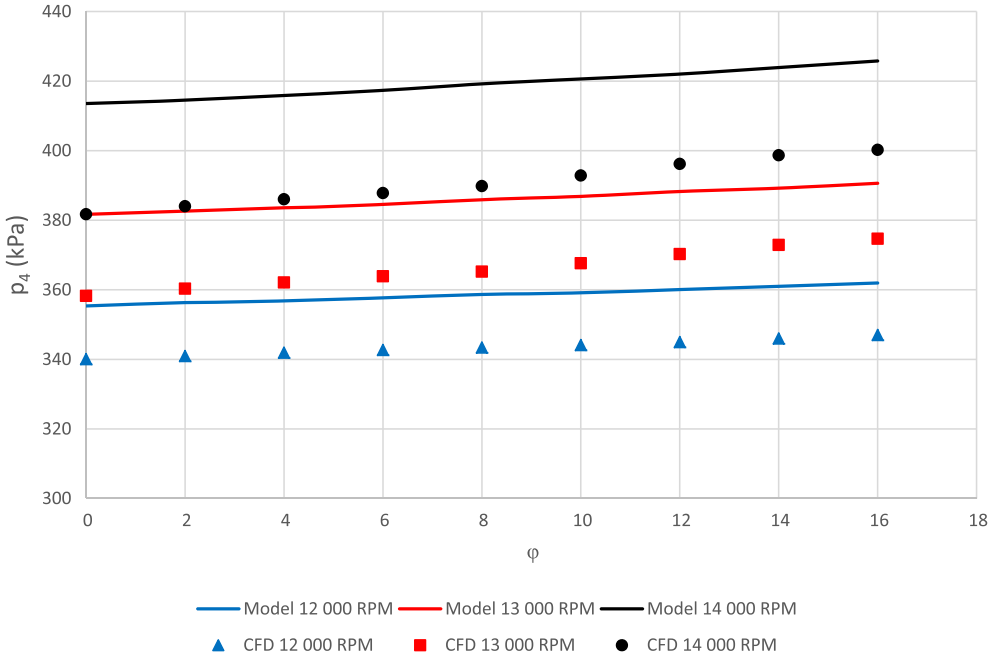

FIGURE 8 Comparison of the diffuser outlet pressure computed by the 1D analytical model the 3D CFX simulation for increasing vane angles φ

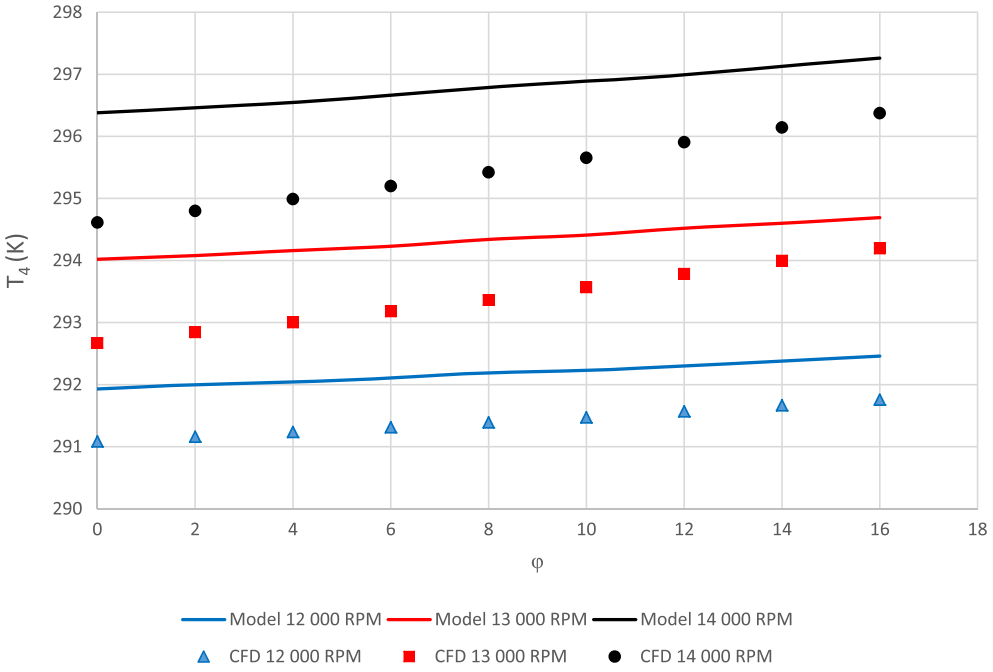

FIGURE 9 Comparison of the diffuser outlet temperature computed by the 1D analytical model the 3D CFX simulation for increasing vane angles φ

The results show a strong similarity between the two sets of results in terms of the variation trend of both the output diffuser temperature and pressure with respect to variations in both the rotational speed and the IGV angle. There is also reasonable agreement in terms of the calculated pressures and velocities; however, the analytical model is seen to over predict the output pressure and temperature. The effect of this is that the pressure ratio (p_4/p_1) is overestimated in the analytical model by between 4% and 8%; and the temperature gain (T_4-T_1) is overestimated by between 4% and 15% for the range of parameters considered here. Although this gives a reasonable estimate of the output pressure and temperature from the diffuser, the overestimate is thought to be associated with the assumption of no pressure losses in the diffuser. The analytical model was rerun with a typical 5% diffuser loss by setting $\varepsilon = 0.95$. This is shown in Figure 10 for the diffuser outlet pressure.

The results in Figure 10 suggest that incorporating the diffuser losses into the model accounts for most of the differences observed in Figure 8, with the percentage difference in the pressure ratio reduced to no more than 2%.

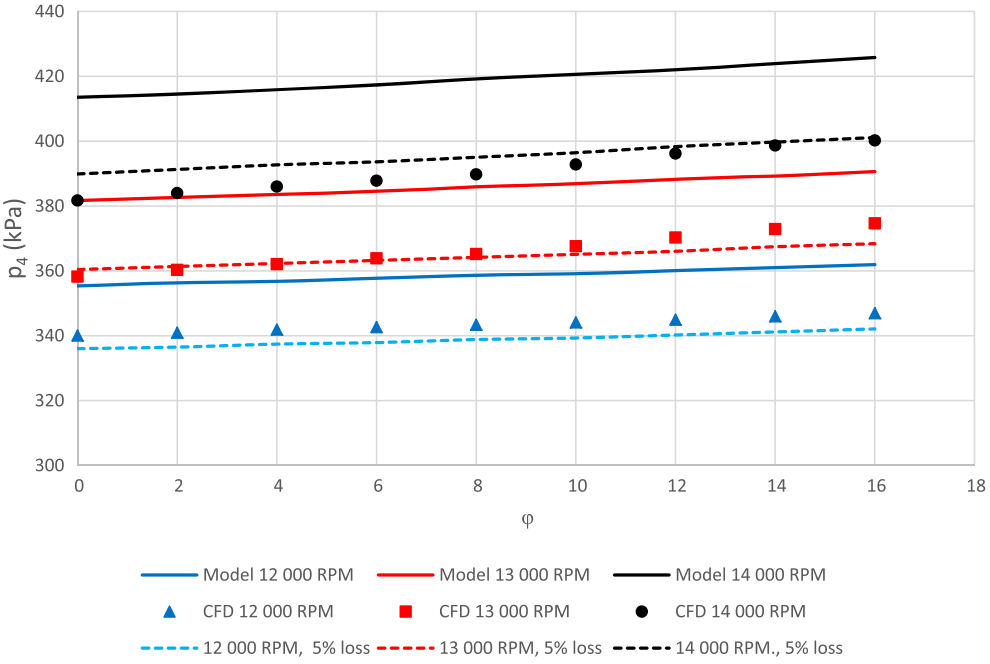

FIGURE 10 Diffuser outlet pressure from the 1D analytical model with a 5% diffuser loss

4 | DISCUSSION

While 3D CFD simulations of a centrifugal compressor will always provide a more detailed description of a compressor performance and enable features such boundary layer development[19] to be investigated, there are many practical applications where a detailed knowledge of the flow through the compressor is not required and this level of detail, along with a small level of accuracy, can be sacrificed for a rapid and robust prediction model like the one presented here. For example, in air-conditioning applications, load requirements can change with the number of people and/or mechanical devices in the conditioned space, as well as changes to the outdoor temperature. In such cases, the 1D model provides a quick and relatively accurate method to determine the effect of changing the IGV angle and/or rotational speed and, hence, determine the appropriate approach to provide the required compressor performance in the most efficient manner.

Here, the model had been limited to relatively low IGV angles, where flow separation is not expected to occur. At larger angles, flow separation and associated eddies will affect the flow entering the impeller region and will invalidate the assumption of Equation (19). In such cases, the 1D model will not give such an accurate approximation of the outlet parameters; however, the separated flow will affect the performance of the compressor and high IGV angles will not produce optimal operating conditions.

Clearly, the performance of a centrifugal compressor depends on details of the impeller geometry, which are not included in the 1D model presented here, such as the curvature of the impeller blades. For this reason, one of the model inputs is the mass flow rate $\dot{m}_0$, at a single, known rotational speed Ω_0 in the absence of IGVs. This makes the model more flexible since it opens up its application to a wide range of centrifugal compressor designs and applications; however, it does require this additional input. In practice, the details can be found from knowledge of an existing system, or manufacturer's data, or even a single CFD simulation. Even if precise data is not available, the model will still give a good representation of the relative effects on the compressor performance of altering the rotational speed and the IGV angle.

Introducing a 5% total pressure drop[23] at the diffuser outlet was shown in Figure 10 to align the 1D model to the CFD simulations within a couple of percent. The nature of such losses is complex and will depend on a number of parameters including the swirl velocity, the rotational speed, the impeller geometry, and the geometry of the diffuser itself. A uniform value of 5% may not be suitable in all cases and will not guarantee a 2% accuracy in the model output. Despite this, the results in Figures 8 and 9 indicate that, even without considering any losses, the 1D model perfumes well; introducing an approximation for the total pressure losses, despite some limitations on using a fixed percentage value, will only act to improve the accuracy of the model.

An important consideration is the range of conditions over which the model can be applied. The aim of the model is to provide a quick, but relatively accurate, method for determining how the compressor reacts to changes in the rotation speed and/or the IGV angle; rather than examining the effect of geometry change, which requires a full CFD

simulations.[19,26] As discussed earlier, features such as the specific geometry of the impeller blades (other than the radial sizes) and unsteady features such as vortex fluctuations are not considered but are captured in the input $\dot{m}_{01}$ for the specific compressor being considered. Since the specifics of any particular compressor is incorporated in this way, it is anticipated that the model will be applicable over a large range of both compressor designs and operating conditions; however, its use will be limited if the operating conditions are varied to such an extent that the compressor enters surge or choke. The impeller blades and angles are assumed to be such that they do not cause any dynamics such as severe flow separation. In the CFD model, the leading edges are modeled to be ellipses of 2:1 ratio.

5 | CONCLUSIONS

A 1D in-line analytical model has been presented for a centrifugal compressor with variable rotational velocity and IGV angles. The model has been implemented in MATLAB and the output compared to 3D CFX simulations. The CFX simulations were used to validate the key assumption in the 1D model and to assess the validity of the 1D model. The model assumptions were found to be valid and the output from the compressor was found to be in good agreement with the CFD results, particularly when diffuser losses were taken into account. The 1D model provides a useful tool for understanding role of the inlet guide vanes and the rotational velocity on the performance of the compressor. It is envisaged that the model will aid operators in determining the best operating conditions to enable centrifugal compressors to be run at their optimal performance in differing scenarios, thus reducing both the running costs of the compressors and their environmental impact.

ACKNOWLEDGEMENTS

Numerical computations were done on the Sciama High Performance Compute (HPC) cluster, which is supported by the ICG, SEPNet, and the University of Portsmouth. The authors wish to thank InnovateUK for financial support provided for this work through the KTP grant (KTP009973).

ORCID

Brett Dewar https://orcid.org/0000-0002-5984-1926

REFERENCES

1. Mohseni A, Goldhahn E, Van den Braembussche RA, Seume JR. Novel IGV designs for centrifugal compressors and their interaction with the impeller. *J Turbomach*. 2011;134(2):021006. https://doi.org/10.1115/1.4003235
2. Liu Y, Tan L, Liu M, Hao Y, Xu Y. Influence of Prewhirl angle and axial distance on energy performance and pressure fluctuation for a centrifugal pump with inlet guide vanes. *Energies*. 2017;10:695. https://doi.org/10.3390/en10050695
3. Qu W, Tan L, Cao S, Wang Y, Xu Y. Numerical investigation of clocking effect on a centrifugal pump with inlet guide vanes. *Engineering Computations*. 2016;33(2):465-481. https://doi.org/10.1108/EC-12-2014-0259
4. Zhou L, Xi G, Cai Y. Experimental study on the influence of diffuser and inlet guide vane for the performance of centrifugal compressor. *Experimental Techniques*. 2008;32(5):26-33. https://doi.org/10.1111/j.1747-1567.2007.00264.x
5. Xiao J, Gu C-G, Shu XW, Gao C. Performance analysis of a centrifugal compressor with adjustable inlet guide vanes. *J Power Eng*. 2006;26(6):804-807.
6. Ishino M, Iwakiri Y, Bessho A, Uchida H. Effects of variable inlet guide vanes on small centrifugal compressor performance. Paper presented at: ASME 1999 International Gas Turbine and Aeroengine Congress and Exhibition - Volume 1: Aircraft Engine; Marine; Turbomachinery; Microturbines and Small Turbomachinery; 1999; Indianapolis, IN. https://doi.org/10.1115/99-GT-157
7. Whitfield AA, Abdullah AH. The performance of a centrifugal compressor with high inlet Prewhirl. Paper presented at: ASME 1997 International Gas Turbine and Aeroengine Congress and Exhibition - Volume 1: Aircraft Engine; Marine; Turbomachinery; Microturbines and Small Turbomachinery; 1997; Orlando, FL. https://doi.org/10.1115/97-GT-182
8. Tan J, Wang X, Qi D, Wang R. The effects of radial inlet with splitters on the performance of variable inlet guide vanes in a centrifugal compressor stage. *Proc IME C J Mech Eng Sci*. 2011;225(9):2089-2105. https://doi.org/10.1177/0954406211407799
9. Zhou L, Fan H-Z, Wei W, Cai Y-H. Experimental and numerical analysis of the unsteady influence of an inlet guide vane. *Proc IME C J Mech Eng Sci*. 2011;226(3):660-680. https://doi.org/10.1177/0954406211415320
10. Cui MM. Unsteady flow around suction elbow and inlet guide vanes in a centrifugal compressor. Paper presented at: ASME Turbo Expo 2004: Power for Land, Sea, and Air - Volume 5: Turbo Expo 2004, Parts A and B; 2004; Vienna, Austria. https://doi.org/10.1115/GT2004-53273
11. Yuchuan W, Lei T, Baoshan Z, ShuLiang C, Binbin W. Numerical investigation of influence of inlet guide vanes on unsteady flow in a centrifugal pump. *Proc IME C J Mech Eng Sci*. 2015;229:3405-3416. https://doi.org/10.1177/0954406215570105

12. Liu M, Tan L, Cao S. Influence of geometry of inlet guide vanes on pressure fluctuations of a centrifugal pump. *J Fluids Eng*. 2018;140:091204. https://doi.org/10.1115/1.4039714
13. Liu M, Tan L, Cao S. A review of prewhirl regulation by inlet guide vanes for compressor and pump. *Proc Inst Mech Eng A J Power Energy*. 2018. https://doi.org/10.1177/0957650918820795
14. Galindo J, Serrano JR, Guardiola C, Cervelló C. Surge limit definition in a specific test bench for the characterization of automotive turbochargers. *Exp Thermal Fluid Sci*. 2006;30(5):449-462. https://doi.org/10.1016/j.expthermflusci.2005.06.002
15. Brandstetter C, Biela C, Kegalj M, Schiffer H-P. PIV-measurements in a transonic compressor test rig with variable inlet guide vanes. Paper presented at: 20th International Symposium on Air Breathing Engines (ISABE); 2011; Gothenburg, Sweden. https://doi.org/10.13140/RG.2.1.5124.2968
16. Jaatinen-Värri A, Turunen-Saaresti T, Röyttä P, Grönman A, Backman J. Experimental study of centrifugal compressor tip clearance and vaneless diffuser flow fields. *Proc Inst Mech Eng A J Power Energy*. 2013;227(8):885-895. https://doi.org/10.1177/0957650913497358
17. Li J, Yin Y, Li S, Zhang J. Numerical simulation investigation on centrifugal compressor performance of turbocharger. *J Mech Sci Technol*. 2013;27(6):1597-1601. https://doi.org/10.1007/s12206-013-0405-3
18. Rinaldi E, Pecnik R, Colonna P. Computational fluid dynamic simulation of a supercritical CO_2 compressor performance map. *J Eng Gas Turbines Power*. 2015;137(7):072602. https://doi.org/10.1115/1.4029121
19. Tiainen J, Jaatinen-Värri A, Grönman A, Backman J. Numerical study of the Reynolds number effect on the centrifugal compressor performance and losses. Paper presented at: ASME Turbo Expo 2016: Turbomachinery Technical Conference and Exposition - Volume 2D: Turbomachinery; 2016; Seoul, South Korea. https://doi.org/10.1115/GT2016-56036
20. Liu Y, Tan L. Spatial–temporal evolution of tip leakage vortex in a mixed-flow pump with tip clearance. *J Fluids Eng*. 2019;141(8):081302. https://doi.org/10.1115/1.4042756
21. Liu Y, Tan L. Tip clearance on pressure fluctuation intensity and vortex characteristic of a mixed flow pump as turbine at pump mode. *Renewable Energy*. 2018;129(Pt A):606-615. https://doi.org/10.1016/j.renene.2018.06.032
22. Hao Y, Tan L. Symmetrical and unsymmetrical tip clearances on cavitation performance and radial force of a mixed flow pump as turbine at pump mode. *Renewable Energy*. 2018;127:368-376. https://doi.org/10.1016/j.renene.2018.04.072
23. Van den Braembussche RA (ed). *Radial Compressor Design and Optimization*. Sint-Genesius-Rode, Belgium: von Karman Institute for Fluid Dynamics.
24. NIST reference fluid thermodynamic and transport properties database (REFPROP): version 10. https://www.nist.gov/srd/refprop
25. Dewar B, Tiainen J, Jaatinen-Värri A, et al. CFD modelling of a centrifugal compressor with experimental validation through radial diffuser static pressure measurement. *Int J Rotating Mach*. 2019;2019:7415263. https://doi.org/10.1155/2019/7415263
26. Dewar BP, Buick JM, Radulovic J, Craemer MR. Design philosophy for multivariable optimisation in centrifugal compressor design. Paper presented at: Symposium on Innovative Simulations in Turbomachinery (ISimT); 2017; Tegernsee, Germany.

How to cite this article: Dewar B, Creamer M, Dotcheva M, Radulovic J, Buick JM. A 1D mean line model for centrifugal compressors with variable inlet guide vanes. *Engineering Reports*. 2019;1:e12027. https://doi.org/10.1002/eng2.12027